Hindawi
Journal of Nanomaterials
Volume 2022, Article ID 5706132, 11 pages
https://doi.org/10.1155/2022/5706132

Research Article

Optimization on Tribological Characteristics of Stir-Casted AA7076/Nano Zirconium Dioxide/Boron Nitride Hybrid Composites by Taguchi Method

S. Shenbaga Ezhil,[1] A. Shanmuganathan,[2] Ganganagunta Srinivas,[3] K. Ashokkumar,[4] Sultan Althahban,[5] S. Mousa,[6] Faez Qahtani,[7] Yosef Jazaa,[8] and Nagaraj Ashok[9]

[1]*Department of Mathematics, Jeppiaar Institute of Technology, Sriperumpudur, 631604 Tamilnadu, India*
[2]*Department of Mechanical Engineering, NIMS University, Jaipur, 303121 Rajasthan, India*
[3]*Department of Physics, University of Technology and Applied Sciences, IBRA, North Al Sharqia Region, Oman 400*
[4]*Department of Mechanical Engineering, Panimalar Engineering College, Varadharajapuram, Chennai-, 600123 Tamilnadu, India*
[5]*Department of Mechanical Engineering, Jazan University, Jazan 82822, Saudi Arabia*
[6]*Faculty of Engineering, Jazan University, Jazan 706, Saudi Arabia*
[7]*Department of Mechanical Engineering, Najran University, Najran-11001, Saudi Arabia*
[8]*Faculty of Engineering, King Khalid University, Saudi Arabia*
[9]*Faculty of Mechanical Engineering, Jimma Institute of Technology, Jimma University, Jimma, Ethiopia 378*

Correspondence should be addressed to Nagaraj Ashok; nagaraj.ashok@ju.edu.et

Received 17 March 2022; Accepted 16 June 2022; Published 18 July 2022

Academic Editor: Palanivel Velmurugan

Copyright © 2022 S. Shenbaga Ezhil et al. This is an open access article distributed under the Creative Commons Attribution License, which permits unrestricted use, distribution, and reproduction in any medium, provided the original work is properly cited.

Aluminum alloys are currently used in a wide variety of industries, and strong aluminum alloys are required for the creation of new components. As a result, multiple scientists are experimenting with various compositions of hybrid aluminum metal matrix composites. The purpose of this experiment was to generate hybridization on aluminum alloy 7076 using stir-casting and nano zirconium dioxide and BN reinforcements. Taguchi's approach was used to optimize the stir-casting process criteria in this investigation. The parameters employed in this investigation were agitation speed, agitation time, and temperature. The chosen constraints are the percentage of reinforcement (0–12%), the agitation speed, the agitation time, and the molten state temperature. We used a wear tester and a Vickers hardness tester to determine the wear and microhardness of the produced stir casting materials. By optimizing wear parameters, the least wear rate is determined.

1. Introduction

Alloys of aluminum have outstanding mechanical qualities and machinability characteristics, as well as the ability to be strengthened by adding the reinforcement elements [1, 2]. The addition of hard ceramic particles improves the alloy materials strength and mechanical qualities, as well as their corrosion resistance, using the AZ91 magnesium alloy with graphite particle accumulation [3–5]. Modern engineering firms have started innovative technology to maintain and thrive in quality at low cost. Manufacturing sectors are continually on the lookout for new materials due to rapid technological advancements and the need for low-cost materials. The tribological and mechanical characteristics of aluminum materials were studied by [6]. Magnesium alloy [7] is infused with graphite at varying volume fraction levels, with the 60 to 100 percent volume fraction resulting in a lower wear rate, and the wear forms is like peeling wear [8]. The basic alloy with 5% graphite may be easily refined and formed into a homogeneous combination.

Stir-casting [9] was employed by [10] to create aluminum hybrid composites using silicon carbide and tungsten carbide. The composites' mechanical strength and wear characteristics are currently being evaluated in-depth in an

experimental study by the scientists [11, 12]. SiC and WC materials are uniformly dispersed into an aluminum alloy for microstructural analysis. Owing to the strong merging of the strengthening particles with the base materials, greater hardness values are tested in all measures. The extensive fusing of the tough materials during the stir-casting process greatly improves the composites' wear resistance [13, 14].

Tests on the wear resistance of Al 6061 with B4C and mica particles were conducted by [15]. The abrasive resistance and COF of stir-casted composite samples were determined by a wear test [16]. Friction stir-casting is used to incorporate 70 m boron carbide and 10 m mica particles. In their research, they employed dry sliding wear test parameters with applying loads of 10, 20, and 30 Newtons. For wear resistance and COF, the AA6061/B4C/Mica composites were superior than the AA6061/B4C composites [17, 18].

Aluminum matrix composites, including those containing SiC and red mud, were examined by [19] using a stir-casting procedure [20]. Studies rely on Taguchi's statistical technique, which favors factors like red mud portion, particles size and weight usage, sliding distance, and speed of movement. In their evaluation of wear loss and coefficient friction, the gliding distance and applied load are the most critical parameters [21, 22]. Red mud was discovered to boost wear resistance by increasing the amount of red sludge and decreasing the load and sliding distance.

By [23], wear on aluminum 2024 alloys with diverse % of fly ash and SiC was examined. Various reinforcing percentages of fly ash and SiC are combined in equal weight fractions (5 percent, 10 percent, and 15 percent). Researchers analyzed L27 orthogonal arrays. The composites' wear resistance rises with rising load and sliding distance [24]. It is clear that when comparing wear test to another factors like sliding duration and percentage of reinforcement, applied load had the greatest impact on all three metrics.

To improve the mechanical characteristics and strength of various alloy materials for reinforcing hare particles, stir-casting was heavily utilized. To prepare a composite, stir-casting method process parameters play a significant role, with each one having an impact on a different character [25]. Composite characteristics have an impact on the final outcome. Alloy alloys must be tested for wear resistance by wear analysis. In most cases, the wear test is performed in a dry environment. Measurement of the hardness of materials can be done using microhardness testing methods. Hardness can be measured more accurately and less destructively with the Vickers test than with other methods [26]. As a result of careful consideration of all relevant aspects and a thorough review of relevant literature, aluminum metal matrix composites were selected for this investigation. For this experiment, we used aluminum alloy 7076 with nano zirconium dioxide (ZrO2) and micron boron nitride reinforcement particles as foundation element. The stir-casting process is used to make hybrid composites, and the process parameters are optimized using the Taguchi method [27–29]. Investigation of AMMC's mechanical and tribological properties will be the key focus of this project. In order to estimate wear rate and assess the hardness value of stir-cast parts, Pin-On Disc equipment and Vickers microhardness are used on the stir-cast composites.

2. Materials

XRF was utilized to determine aluminum alloy's constituent makeup (AA7076). Because of its great abrasion resistance, exceptional strength, superior ductility, and outstanding Heat and electrical characteristics, aluminum alloy 7076 was chosen for this study. They are originally wrought alloys, and they have an extremely machinable character. AA7076 alloy is used to build highly stressed components for machines, mobile gadget, hydraulic valves, and air wing parts [30]. This study's reinforced particles are made from nano zirconium dioxide (30 nm) and micron boron nitride (50 μm) as boron nitride is being used as a lubricant in paints, cosmetics, pencil lead, and dental cement. Reinforced hybrid particles with high tensile strength are mixed into the base material to boost its tensile strength. In materials such as aluminum alloy AA7076, components included in the basic material are listed in Table 1.

3. Experimental Procedure

A stir-casting technique is used to first create an aluminum alloy and reinforced particles, which may then be controlled by varying various process parameters. Further testing will include a wear test and a microhardness test. Using the stir-casting procedure, the following variables and their corresponding values are shown in Table 2. Four constraints were employed to cast the AMMC, such as reinforcement percentage, agitation speed (rpm), agitation duration (min), and melting temperature. The L16 OA was successfully completed. Blending base materials and reinforcement particles together via liquid state stir-casting are used in this study. The 5 kilogram crucible is filled with sliced AA7076 plates, and the crucible is then placed into the stir casting machine. The aluminum alloy is melted by heating the crucible to various temperatures (700 °C, 750 °C, 800 °C, and 850 °C). Nano zirconium dioxide and boron nitride are cooked in the muffle furnace simultaneously, and their weight ratios are maintained although their percentage levels differ. In addition, the stir-casting machine's stirrer and varied agitation rates effectively combine the base material with reinforced particles (450, 500, 550, and 600 rev/min). A variety of agitation time periods (15, 20, 25, and 30 minutes) were used to ensure that the composites were thoroughly mixed. Finally, the crucible's molten contents were poured into the dies to produce the desired forms.

3.1. Wear Test. As a result of this process, the wear test samples are cast using parameters like 8 percent reinforcement, 600 RPM, and a molten temperature of around 850 °C. Amount of reinforcement, applying load (Newtons), disc speed (meter/sec), and sliding distance are a few of the features stated in Table 3. A wide range of values can be assigned to each of the parameters. The DUCOM model was put through a rigorous wear test using a Pin-On-Disc system, which measures the wear on the specimens by sliding them across a dry surface. The specimens were 40 mm long and 12 mm diameter, and they were all put through a wear test in accordance with ASTM G99's standard protocol.

Table 1: Chemical composition of AA7076.

Material	Percentage of composition
Copper	1.0
Iron	0.58
Magnesium	2.0
Manganese	0.3
Silicon	0.4
Zinc	7.0
Titanium	0.2
Aluminum	Balance

Table 2: specifications and levels for the stir-casting process.

Specifications		Levels			
		1	2	3	4
Percentage of reinforcement	(%)	0	4	8	12
Agitation speed	(rev/min)	450	500	550	600
Agitation time	(min)	15	20	25	30
Temperature at molten stage	(°C)	700	750	800	850

Table 3: Wear test process specifications.

S. No	Specifications	Level 1	Level 2
1.	Percentage of reinforcement	0	4
2.	Applying load (Newtons)	15	25
3.	Disc speed (meter/seconds)	1.0	1.5
4.	Sliding distance (mm)	1000	1200

On behalf of the L16 orthogonal array configuration, each specimen was examined using a different set of parameters.

3.2. Vickers Microhardness Test. One of the optical measurement setups is Vickers microhardness testing, which uses specimens produced in accordance with ASTM standards. Diamond indenter was utilized to make an imprint on the sample's surface and apply a small load to determine the specimen's hardness value. When performing the Vickers hardness test, the normal load variation ranges from 10 gm to 1 kgf; however, in this instance, just a 0.5 kgf weight was used.

4. Results and Discussion

4.1. Wear Test. 0.238 mm^3/m of lowest wear rate was obtained with a 12 percent reinforcement contribution, 25 Newton applied load, 1.5 meter/sec disc speed, and 1200 meter sliding speed (see Table 4 for an experimental overview of the wear test).

It can be seen here that there is a response table for wear test methods in Table 5 and a response table for wear test S/N ratios in Table 6. Experiment design is employed to transform all of the input data into wear test mean and S/N ratio values. The sliding distance, applied stress, and disc speed were all strongly influenced by the percentage of reinforcement in the wear test. It was determined that 12 percent reinforcement, 25 Newton applied stress, 1.5 meter/sec disc speed, and 1200 mm sliding speed were the best parameters for the wear test.

Wear test main effects plots for mean and S/N ratios are shown in Figures 1 and 2. Due to the lack of reinforcement, the specimen's wear rate was significantly higher. Increasing the reinforcing percentage also helped to reduce the wear rate. Finally, the greater reinforcing percentage (12%) had the lowest wear rate. Applying a greater applied load

Table 4: Wear test summary.

Reinforcement	Applying load	Speed on disc	Sliding distance	Rate of wear
%	(Newtons)	(meter/sec)	(mm)	(mm^3/m)
0	15	1.0	1000	.568
0	25	1.5	1200	.384
0	35	2.0	1400	.801
0	45	2.5	1600	.835
4	15	1.0	1000	.558
4	25	1.5	1200	.712
4	35	2.0	1400	.426
4	45	2.5	1600	.835
8	15	1.0	1000	.751
8	25	1.5	1200	.504
8	35	2.0	1400	.409
8	45	2.5	1600	.599
12	15	1.0	1000	.686
12	25	1.5	1200	.238
12	35	2.0	1400	.351
12	45	2.5	1600	.296

Table 5: Response table for average.

Level	Percentage of reinforcement	Applying load (Newtons)	Speed on disc (meter/sec)
1	0.6415	0.6325	0.4868
2	0.6195	0.4468	0.4638
3	0.6477	0.4870	0.6423
4	0.3840	0.6265	0.6000
Delta	0.2601	0.1796	0.1826
Rank	1	3	4500

Table 6: S/N ratios response table.

Level	Percentage of reinforcement	Applying load (Newton)	Speed on disc (meter/sec)
1	4.249	4.041	6.749
2	4.428	7.681	6.893
3	5.461	6.739	4.832
4	9.083	4.761	4.748
Delta	4.834	3.640	2.145
Rank	1	3	4.493

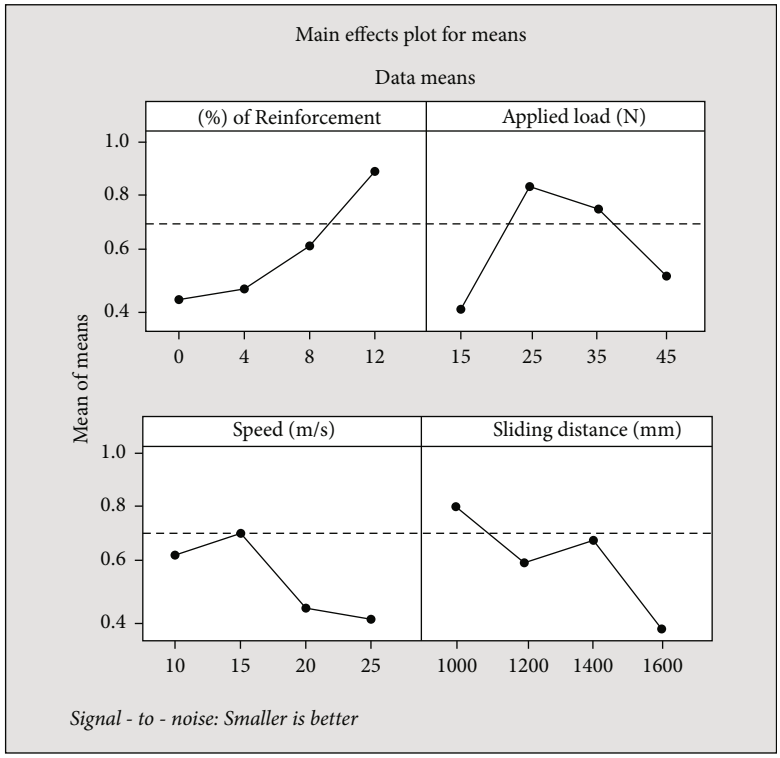

Figure 1: Average plot effects for wear test.

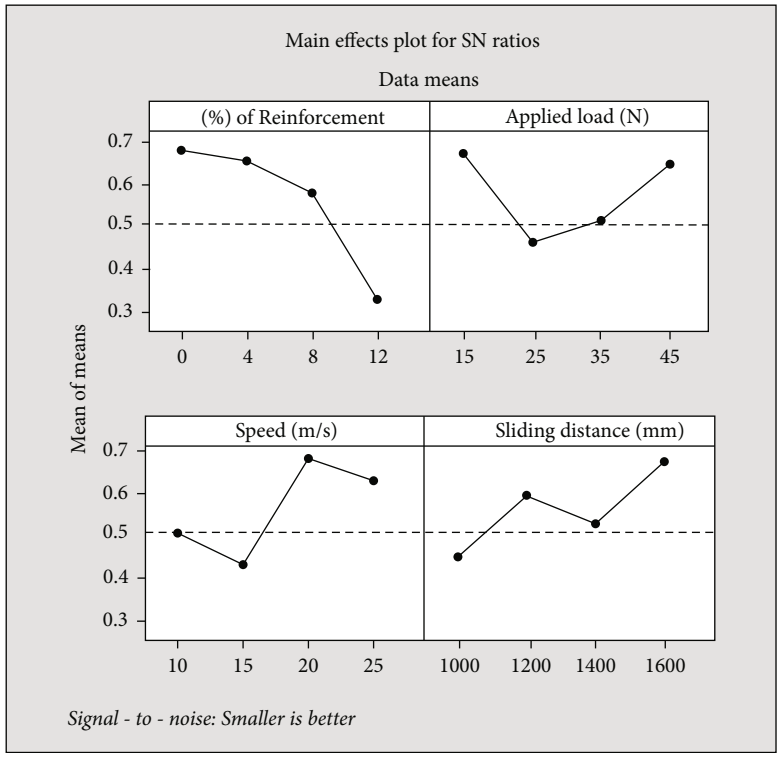

Figure 2: S/N ratio plot effects for wear test.

(25 N) causes the wear rate to drop rapidly at first, but when the applied force is increased, the wear rate rises again. The wear rate increased once again when the applied force was raised from 25 N to 45 N. At 1.5 meter/sec disc speed, wear rate was at its lowest; as disc speed increased, the wear rate increased as well.

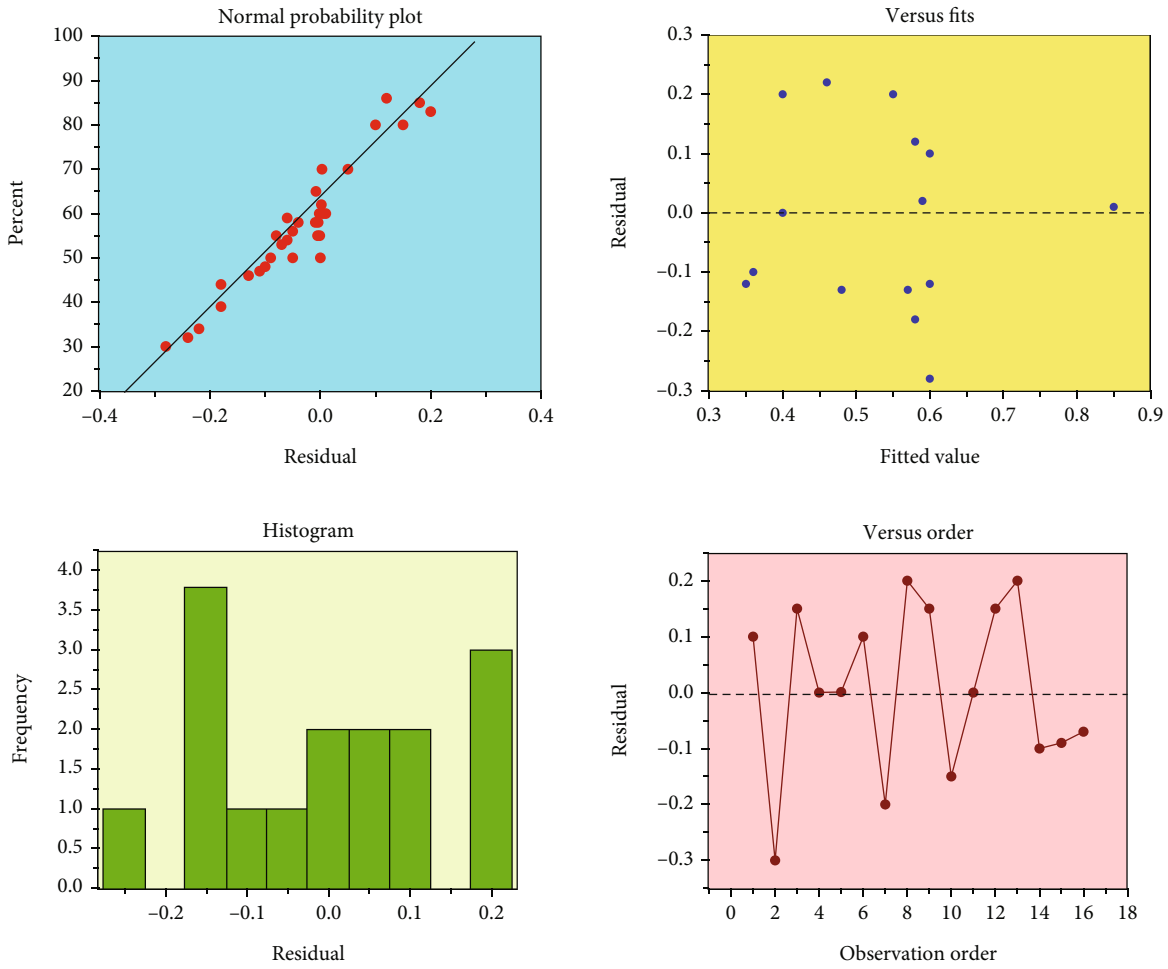

Figure 3: Wear rate residual plots.

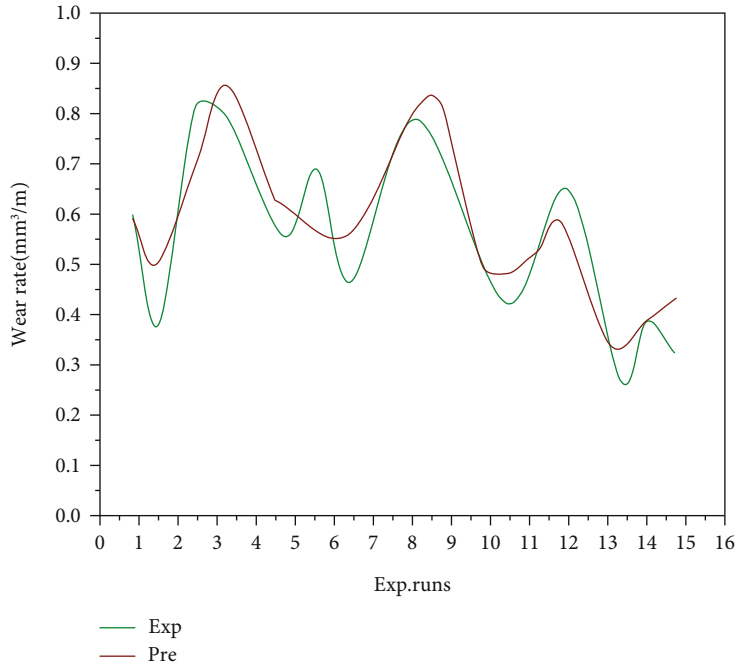

Figure 4: Experiment numbers vs wear rate.

Table 7: VHN summary.

Experiment number	Percentage of reinforcement (%)	Agitation speed (rev/min)	Agitation time (min)	Temperature at molten state (°C)	Vickers hardness number (VHN)
1	0	450	15	700	112
2	0	500	20	750	91
3	0	550	25	800	116
4	0	600	30	850	114
5	4	450	15	800	118
6	4	500	20	850	112
7	4	550	25	700	119
8	4	600	30	750	121
9	8	450	15	850	124
10	8	500	20	800	125
11	8	550	25	750	121
12	8	600	30	700	118
13	12	450	15	750	125
14	12	500	20	700	120
15	12	550	25	800	126
16	12	600	30	850	119

Table 8: Average response table for VHN.

Level	% of reinforcement	Agitation speed (rpm)	Agitation time (min)	Molten temperature (C)
1	108	116	112	113
2	114	112	112	115
3	118	117	117	116
4	119	115	118	115
Delta	12.0	6.2	5.4	3.0
Rank	1	2	3	4

Table 9: S/N ratio response table.

Level	Reinforcement (%)	Agitation speed (rev/min)	Agitation time (min)	Temperature at molten state (°C)
1	41.2	42.6	41.02	42.8
2	41.11	40.88	41.94	41.32
3	41.42	41.30	41.25	41.0
4	41.47	41.18	0.21	36
Delta	0.89	0.42	41	42
Rank	1	2	3	4

Figure 3 shows the wear rate residual graphs. As shown in the residual plot, each parameter has a direct impact on the other three. There are sixteen points on a normal probability plot, but only some of them are close to line, which can be seen in wear rate, which was found by directing accurate experimentations. It is possible to accurately measure the given parameters using the fit plot, as the points are distributed uniformly. They are all very close to each other in a histogram display of the data. There was a simultaneous positive and negative crossing of the mean line plotting the dots in a specific sequence. As a result of these circumstances, the experiment was executed flawlessly, and the parameters were effectively utilized.

Figure 4 depicts the wear test's experimental runs compared to the wear rate. The experimental and anticipated values are analyzed from the wear test. There were just a few values that were closer to or even crossed the projected levels in the sixteen experiments.

4.2. Vickers Microhardness Test. The Vickers microhardness test yielded a maximum hardness of 126 VHN, as shown in Table 7. The highest hardness was impacted by the criteria

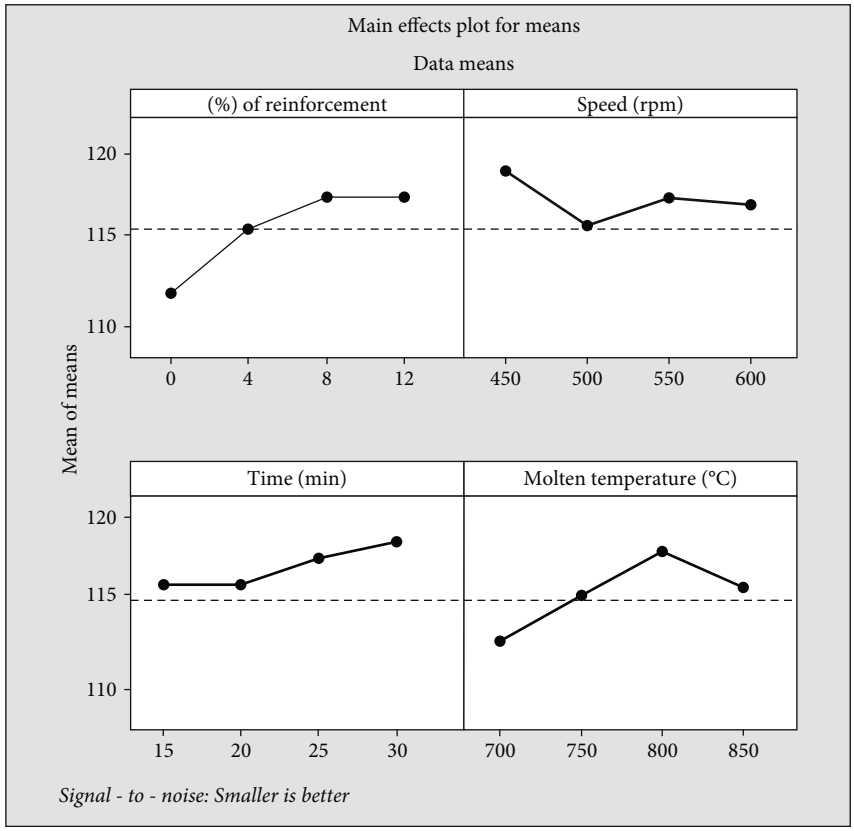

Figure 5: Main effects plot for average.

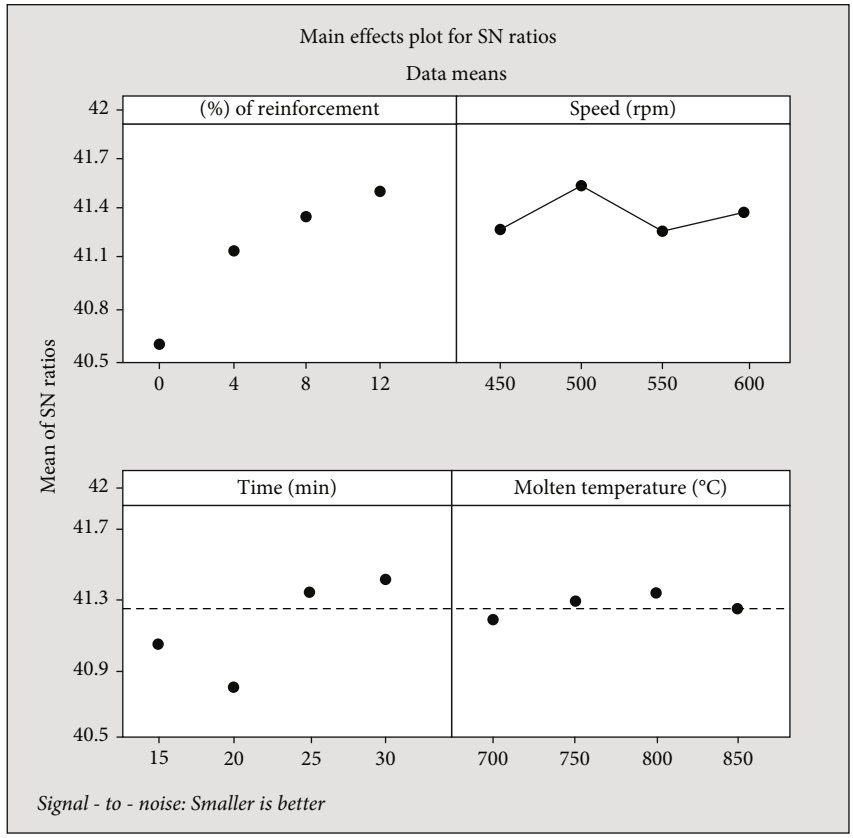

Figure 6: S/N ratios main plot effects.

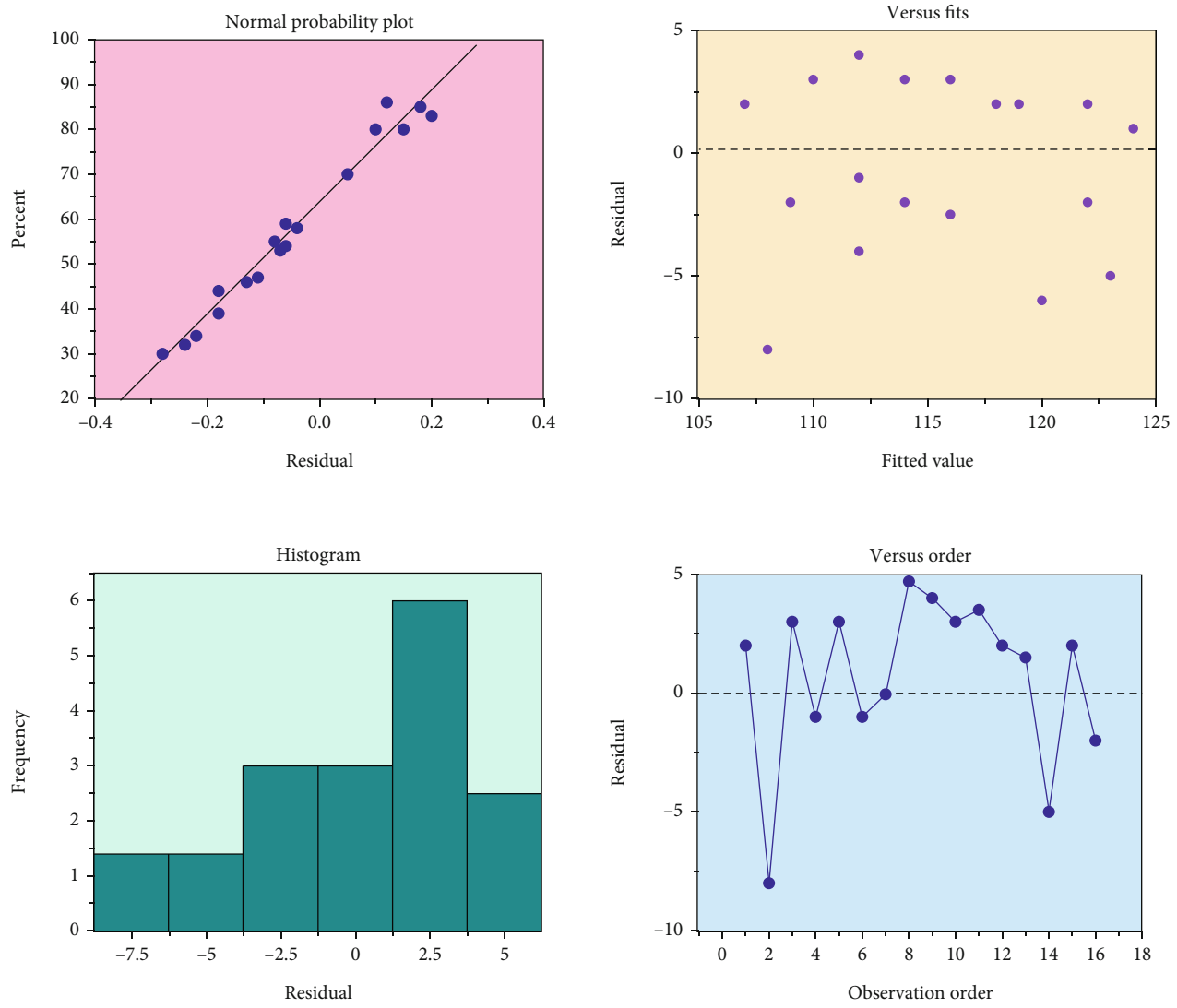

Figure 7: Residual plots for Vickers hardness.

12 percent reinforcement, 550 rpm agitation speed, 25 minute agitation time, and a molten temperature of 800° C. Through DoE, Vickers hardness test results are transformed into mean as in Table 8 and S/N ratios as in Table 9. Percentage of reinforcement was the most important factor in Vickers hardness test after agitation speed, agitation time, and temperature at molten state. 12 percent reinforcement, 550 rpm agitation speed, 25 minute intervals, and 800 °C temperature were found to be the appropriate Vickers hardness test settings.

Figures 5 and 6 show the Vickers hardness test's main effects plot for average and S/N ratios. Microhardness value was raised by increasing the reinforcing percentage. Finally, the larger proportion of reinforcement (12 percent) resulted in the greatest microhardness possible. An increase of 500 rpm agitation speed reduced the value of microhardness rapidly. An increase in microhardness was achieved by increasing the speed of rotation from 500 to 550 revolutions per minute. In the agitation time stage, rising the agitation time steadily raised the microhardness value; 25 minutes supplied the maximum hardness values. Microhardness increased as the molten temperature rose, starting at the lowest level and continuing to rise as the temperature grew. As a last point, the microhardness values reached their peak at 800 °C. Vickers hardness residual graphs are shown in Figure 7. The microhardness level and parameters' influence on it can be seen clearly in a single observation in the residual plot.

All sixteen points on the typical probability plot lie on the probability line, with only a few closer to the line, and this may be recreated experimentally by manipulating the microhardness. There is no variation in points in the fit plot, which means that under the parameters set, the response values are perfect. All of the rectangular boxes in the histogram plot are so close to one another that they are touching. There were no points in the order plot that did not cross the mean line simultaneously, either favorably or negatively. As a result of these settings, the testing was passed out in an outstanding manner, and the criteria used were effective. Experimental runs versus Vickers microhardness are

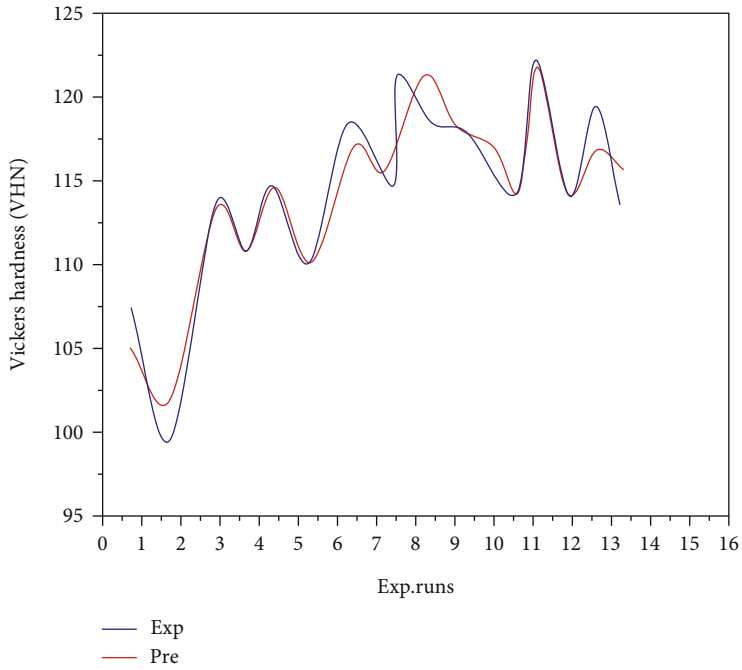

Figure 8: Experimental runs versus Vickers microhardness.

depicted in Figure 8. The experimental and projected results are compared using the Vickers microhardness test. All sixteen experimental runs yielded data that was within the predicted range, although a few were even closer and crossed it.

5. Conclusions

Stir-casting was used to create hybrid composites comprising aluminum alloy 7076 with nano zirconium dioxide and boron nitride (AMCs). In addition, Pin-On-Disc with Taguchi analysis was used to conduct the wear test. In the end, the wear worn-out surfaces and Vickers microhardness were rigorously evaluated for damage. Finally, the experiment's conclusion and results were shown as follows:

(i) When it came to a test of how much of a factor reinforcement play, it was shown to have a 12% impact, with the applied load being 25 N and disc speed being 1.5 m/s, as well as the sliding speed being 1200 m. 12 percent reinforcement, 25 N load, 1.5 m/s disc speed, and 1200 m sliding speed were found to be the optimal parameters for the wear test

(ii) The lowest level of load applied and the highest level of strengthening were shown to have the lowest wear rate in the surface plot study. In addition, the least amount of disc speed and the least amount of applied load provided the least amount of wear rate. For a decreased wear rate, a correlation was found between the min sliding distance and the max reinforcement percentage

(iii) The maximum Vickers microhardness was reported as 126 VHN during the testing process. The parameters of 12 percent reinforcement, agitation speed of 550 rpm, agitation period of 25 minutes, and molten temperature of 800 °C had the greatest impact on the highest hardness values produced. The ideal Vickers hardness test parameters were discovered to be 12 percent reinforcement, agitation speed of 550 rpm, agitation period of 25 minutes, and molten temperature of 800 °C

(iv) The higher reinforcement percentage and moderate agitation speed provided outstanding microhardness, as seen by the contour plot analysis. In addition, the greatest hardness was found to be associated with lower agitation speeds and longer agitation times. Finally, the highest hardness value was found to be a combination of a long agitation period and a moderate molten temperature

Data Availability

The data used to support the findings of this study are included within the article. Further data or information is available from the corresponding author upon request.

Conflicts of Interest

The authors declare that there is no conflict of interest regarding the publication of this article.

Acknowledgments

The authors appreciate the supports from Jimma Institute of Technology, Jimma University, Ethiopia, for the research and preparation of the manuscript. The author thankfully acknowledge the funding provided by Scientific Research

Deanship, King Khalid University, Abha, Kingdom of Saudi Arabia, under the grant number R.G.P.1/267/43.

References

[1] V. Mohanavel and M. Ravichandran, "Influence of AlN particles on microstructure, mechanical and tribological behaviour in AA6351 aluminum alloy," *Materials Research Express*, vol. 6, no. 10, article 106557, 2019.

[2] D. Bandhu, A. Thakur, R. Purohit, R. K. Verma, and K. Abhishek, "Characterization & evaluation of Al7075 MMCs reinforced with ceramic particulates and influence of age hardening on their tensile behavior," *Journal of Mechanical Science and Technology*, vol. 32, no. 7, pp. 3123–3128, 2018.

[3] P. V. Reddy, P. R. Prasad, D. M. Krishnudu, and E. V. Goud, "An investigation on mechanical and wear characteristics of Al 6063/TiC metal matrix composites using RSM," *Journal of Bio- and Tribo-Corrosion*, vol. 5, no. 4, pp. 1–10, 2019.

[4] R. S. Bhatia, "An experimental analysis of aluminium metal matrix composite using Al 2 O 3/B 4 C/Gr particles," *International Journal of Advanced Research in Computer Science*, vol. 8, no. 4, 2017.

[5] A. P. Reddy, P. V. Krishna, and R. N. Rao, "Tribological behaviour of Al6061–2SiC-xGr hybrid metal matrix nanocomposites fabricated through ultrasonically assisted stir casting technique," *Silicon*, vol. 11, no. 6, pp. 2853–2871, 2019.

[6] V. Mohanavel, K. Rajan, and M. Ravichandran, "Synthesis, characterization and properties of stir cast AA6351-aluminium nitride (AlN) composites," *Journal of Materials Research*, vol. 31, no. 24, pp. 3824–3831, 2016.

[7] J. A. Jeffrey, S. S. Kumar, P. Hariharan, M. Kamesh, and A. M. Raj, "Production and assessment of AZ91 reinforced with nano SiC through stir casting process," *Materials Science Forum*, vol. 1048, pp. 9–14, 2022.

[8] Z. Leng, T. Li, X. Wang, S. Zhang, and J. Zhou, "Effect of graphite content on the conductivity, wear behavior, and corrosion resistance of the organic layer on magnesium alloy MAO coatings," *Coatings*, vol. 12, no. 4, p. 434, 2022.

[9] M. L. Bharathi, S. Adarsh Rag, L. Chitra et al., "Investigation on wear characteristics of AZ91D/nanoalumina composites," *Journal of Nanomaterials*, vol. 2022, Article ID 2158516, 9 pages, 2022.

[10] K. Palanikumar, S. E. Rajkumar, and K. Pitchandi, "Influence of primary B4C particles and secondary mica particles on the wear performance of Al6061/B4C/Mica hybrid composites," *Journal of Bio- and Tribo-Corrosion*, vol. 5, no. 3, 2019.

[11] S. Aribo, A. Fakorede, O. Ige, and P. Olubambi, "Erosion-corrosion behaviour of aluminum alloy 6063 hybrid composite," *Wear*, vol. 376-377, pp. 608–614, 2017.

[12] K. Hemalatha, C. James, L. Natrayan, and V. Swamynadh, "Analysis of RCC T-beam and prestressed concrete box girder bridges super structure under different span conditions," *Materials Today: Proceedings*, vol. 37, pp. 1507–1516, 2021.

[13] V. Mohanavel, S. S. Kumar, V. Sivaraman, V. K. Girish, and M. Ravichandran, "Tungsten Carbide Particulate Reinforced AA7050 Aluminum Alloy Composites Fabricated by Liquid State Processing," in *AIP Conference Proceedings*, vol. 2283, AIP Publishing LLC, 2020no. 1, Article ID 020087.

[14] S. K. Chourasiya, G. Gautam, and D. Singh, "Mechanical and tribological behavior of warm rolled Al-6Si-3graphite self lubricating composite synthesized by spray forming process," *Silicon*, vol. 12, no. 4, pp. 831–842, 2020.

[15] J. Singh and A. Chauhan, "Investigations on dry sliding frictional and wear characteristics of SiC and red mud reinforced Al2024 matrix hybrid composites using Taguchi's approach," *Proceedings of the Institution of Mechanical Engineers, Part L: Journal of Materials: Design and Applications*, vol. 233, no. 9, pp. 1923–1938, 2019.

[16] V. Paranthaman, K. S. Sundaram, and L. Natrayan, "Influence of SiC particles on mechanical and microstructural properties of modified interlock friction stir weld lap joint for automotive grade aluminium alloy," *Silicon*, vol. 14, no. 4, pp. 1617–1627, 2022.

[17] S. Banerjee, S. Poria, G. Sutradhar, and P. Sahoo, "Dry sliding tribological behavior of AZ31-WC nano-composites," *Journal of Magnesium and Alloys*, vol. 7, no. 2, pp. 315–327, 2019.

[18] W. Yu, D. Chen, L. Tian, H. Zhao, and X. Wang, "Self-lubricate and anisotropic wear behavior of AZ91D magnesium alloy reinforced with ternary Ti2AlC MAX phases," *Journal of Materials Science and Technology*, vol. 35, no. 3, pp. 275–284, 2019.

[19] V. B. Kurapati, R. Kommineni, and S. Sundarrajan, "Statistical analysis and mathematical modeling of dry sliding wear parameters of 2024 aluminium hybrid composites reinforced with fly ash and SiC particles," *Transactions of the Indian Institute of Metals*, vol. 71, no. 7, pp. 1809–1825, 2018.

[20] S. Koksal, F. Ficici, R. Kayikci, and O. Savas, "Experimental optimization of dry sliding wear behavior of in situ AlB_2/Al composite based on Taguchi's method," *Materials and Design*, vol. 42, pp. 124–130, 2012.

[21] S. V. Alagarsamy, R. Balasundaram, M. Ravichandran, V. Mohanavel, A. Karthick, and S. S. Devi, "Taguchi approach and decision tree algorithm for prediction of wear rate in zinc oxide-filled AA7075 matrix composites," *Surface Topography: Metrology and Properties*, vol. 9, no. 3, article 035005, 2021.

[22] S. E. Rajkumar, K. Palanikumar, and P. Kasiviswanathan, "Influence of mica particles as secondary reinforcement on the mechanical and wear properties of Al/B4C/mica composites," *Materials Express*, vol. 9, no. 4, pp. 299–309, 2019.

[23] L. Natrayan, V. Sivaprakash, and M. S. Santhosh, "Mechanical, microstructure and wear behavior of the material AA6061 reinforced SiC with different leaf ashes using advanced stir casting method," *International Journal of Engineering and Advanced Technology*, vol. 8, pp. 366–371, 2018.

[24] A. Pai, S. S. Sharma, R. E. D'Silva, and R. G. Nikhil, "Effect of graphite and granite dust particulates as micro-fillers on tribological performance of Al 6061-T6 hybrid composites," *Tribology International*, vol. 92, pp. 462–471, 2015.

[25] V. Paranthaman, K. Shanmuga Sundaram, and L. Natrayan, "Effect of silica content on mechanical and microstructure behaviour of resistance spot welded advanced automotive TRIP steels," *Silicon*, vol. 14, no. 7, pp. 3429–3438, 2022.

[26] S. J. S. Chelladurai, R. Arthanari, K. Krishnamoorthy, K. S. Selvaraj, and P. Govindan, "Investigation of the mechanical properties of a squeeze-cast LM6 aluminium alloy reinforced with a zinc-coated steel-wire mesh," *Materiali in Tehnologije*, vol. 52, no. 2, pp. 125–131, 2018.

[27] M. Uthayakumar, S. Aravindan, and K. Rajkumar, "Wear performance of Al-SiC-B_4C hybrid composites under dry sliding conditions," *Materials and Design*, vol. 47, pp. 456–464, 2013.

[28] R. Pandiyarajan, P. Maran, S. Marimuthu, and K. C. Ganesh, "Mechanical and tribological behavior of the metal matrix composite AA6061/ZrO 2/C," *Journal of Mechanical Science and Technology*, vol. 31, no. 10, pp. 4711–4717, 2017.

[29] J. Singh and A. Chauhan, "Overview of wear performance of aluminium matrix composites reinforced with ceramic materials under the influence of controllable variables," *Ceramics International*, vol. 42, no. 1, pp. 56–81, 2016.

[30] C. Wang, K. Deng, and Y. Bai, "Microstructure, and mechanical and wear properties of Grp/AZ91 magnesium matrix composites," *Materials*, vol. 12, no. 7, p. 1190, 2019.